British Journal of Pharmacology

British Journal of Pharmacology (2016) **173** 2390–2401 2390

RESEARCH PAPER

Neutrophil maturation rate determines the effects of dipeptidyl peptidase 1 inhibition on neutrophil serine protease activity

Correspondence Philip Gardiner, AstraZeneca, Pepparedsleden 1, Mölndal, 431 83, Sweden. E-mail: philip.gardiner@astrazeneca.com

Received 1 July 2015; **Revised** 1 April 2016; **Accepted** 20 April 2016

P Gardiner[1], C Wikell[1], S Clifton[2], J Shearer[2], A Benjamin[3] and S A Peters[1,4]

[1]AstraZeneca, Mölndal, Sweden, [2]BioFocus, A Charles River Company, UK, [3]AstraZeneca, Cheshire, UK, and [4]Merck Serono R&D, Darmstadt, Germany

BACKGROUND AND PURPOSE

Neutrophil serine proteases (NSPs) are activated by dipeptidyl peptidase 1 (DPP1) during neutrophil maturation. The effects of neutrophil turnover rate on NSP activity following DPP1 inhibition was studied in a rat pharmacokinetic/pharmacodynamic model.

EXPERIMENTAL APPROACH

Rats were treated with a DPP1 inhibitor twice daily for up to 14 days; NSP activity was measured in onset or recovery studies, and an indirect response model was fitted to the data to estimate the turnover rate of the response.

KEY RESULTS

Maximum NSP inhibition was achieved after 8 days of treatment and a reduction of around 75% NSP activity was achieved at 75% *in vitro* DPP1 inhibition. Both the rate of inhibition and recovery of NSP activity were consistent with a neutrophil turnover rate of between 4–6 days. Using human neutrophil turnover rate, it is predicted that maximum NSP inhibition following DPP1 inhibition takes around 20 days in human.

CONCLUSIONS AND IMPLICATIONS

Following inhibition of DPP1 in the rat, the NSP activity was determined by the amount of DPP1 inhibition and the turnover of neutrophils and is thus supportive of the role of neutrophil maturation in the activation of NSPs. Clinical trials to monitor the effect of a DPP1 inhibitor on NSPs should take into account the delay in maximal response on the one hand as well as the potential delay in a return to baseline NSP levels following cessation of treatment.

Abbreviations

CatG, cathepsin G; DPP1, dipeptidyl peptidase 1; NE, neutrophil elastase; NSP, neutrophil serine protease; PPB, plasma protein binding; PR3, proteinase 3

Table of Links

TARGETS	
Enzymes	
DPP1	Cathepsin G
Neutrophil elastase	Proteinase 3

This Table lists key protein targets in this article that are hyperlinked to corresponding entries in http://www.guidetopharmacology.org, the common portal for data from the IUPHAR/BPS Guide to PHARMACOLOGY (Southan *et al.*, 2016), and are permanently archived in the Concise Guide to PHARMACOLOGY 2015/16 (Alexander *et al.*, 2015).

DOI:10.1111/bph.13515

Introduction

Inflammatory diseases of the lung, such as COPD, acute lung injury and cystic fibrosis, are characterized by an over abundance of neutrophils in the lung (Korkmaz *et al.*, 2010). Neutrophils have a central role in the inflammatory process and are the first cells that are recruited to the site of inflammation where they destroy pathogens via phagocytosis and by production of reactive oxygen species and antimicrobial proteins such as neutrophil serine proteases (NSPs) (Keatings *et al.*, 1996; Korkmaz *et al.*, 2010). Thus, because the neutrophil is an important disease modulating cell, it can be targeted to reduce the neutrophil-driven component of inflammatory disease (Fox *et al.*, 2010; Wright *et al.*, 2010).

Neutrophilic inflammation can result in high levels of NSPs (Stockley, 1994). NSPs are stored in azurophilic granules within the neutrophil and are released in response to invading pathogens as part of the pro-inflammatory response (Korkmaz *et al.*, 2010). However, in diseases with chronic neutrophilic lung inflammation, such as COPD, these otherwise beneficial effects are over emphasized, leading to lung tissue damage (Fujita *et al.*, 1990; Sinden *et al.*, 2014). The NSPs neutrophil elastase (NE), cathepsin G (CatG) and proteinase 3 (PR3) are activated by the lysosomal cysteine protease dipeptidyl peptidase 1 (DPP1) [also known as cathepsin C (CatC)] (Guay *et al.*, 2010) during the promyelocyte stage of neutrophil maturation in the bone marrow by removal of an amino terminal dipeptide (Fouret *et al.*, 1989; McGuire *et al.*, 1993). The activated NSPs are then packaged in granules before the mature neutrophils are released from the bone marrow into the blood circulation, a process that takes several days in man. The turnover rate of human neutrophils has been estimated to be 5 to 7 days (Dancey *et al.*, 1976; Friberg *et al.*, 2002; Pillay *et al.*, 2010; Kolaczkowska and Kubes, 2013). Therefore, drugs that aim to combat an over-abundance of NSPs by inhibiting DPP1 will act on the maturing neutrophil during the promyelocyte stage in the bone marrow.

The focus of the work presented here was to relate the turnover of neutrophils in the rat to the NE, CatG and PR3 activities in the bone marrow and the circulating cells following treatment with a DPP1 inhibitor. As part of a model-based drug development approach (Lalonde *et al.*, 2007; Milligan *et al.*, 2013) that integrates preclinical modelling into clinical study design and decision-making, the primary objectives were (i) to confirm that the dynamic change in NSP activity was consistent with the neutrophil turnover rate in the rat and (ii) to apply the observed pharmacokinetic/pharmacodynamic relationship to a clinical phase 1 study program. In particular, from a safety as well as an efficacy perspective, it was considered important to establish the period of treatment that would be required in the phase 1 study to reach maximum inhibition of circulating NSPs and the likely duration of this effect on cessation of treatment. In order to fulfil these objectives, two potent DPP1 inhibitors known as AstraZeneca (AZs) 1 and 2 were chosen as tool compounds. AZ1 and AZ2 had previously been identified as lead compounds in a DPP1 drug development programme within AstraZeneca (Furber *et al.*, 2014).

Methods

Animals

All *in vivo* work was subject to internal ethical review and conducted in accordance with Home Office requirements under the Animals Scientific Procedures Act (1986). All studies involving animals are reported in accordance with the ARRIVE guidelines for reporting *in vivo* experiments (Kilkenny *et al.*, 2010; McGrath and Lilley, 2015). Male Sprague Dawley rats (Charles River for onset studies and pharmacokinetic (PK) study and Harlan UK Ltd for the recovery study) weighing 200–400 g were used in the different studies. Upon arrival, animals were randomly assigned to a treatment group and were then allowed to acclimatize to their new environment for at least 5 days before use in the study. The animals were housed in solid-bottomed cages, with bedding and enrichment and with free access to food and water. Animal rooms were kept at a constant temperature of 21 ± 2°C and relative humidity of 55 ± 10% with a 12 h light/dark cycle. Pharmacodynamic (PD) – onset 1, $n = 8$ in all groups; onset 2, $n = 8$ in all treated groups and $n = 10$ in the vehicle group; and recovery, $n = 10$ in all groups. PK – AZ1, oral dose $n = 4$, intravenous (IV) dose $n = 12$; and AZ2, oral dose $n = 4$, IV dose $n = 4$. A total number of 182 rats were used in the experiments described.

PK studies in the rat

PK parameters used in PD modelling and dose setting were determined following IV and oral dosing at 1 and 3 $mg \cdot kg^{-1}$ respectively. The dose of test compound administered was calculated by the weight difference of the dosing syringe before and after administration. Following dose administration, serial blood samples (200–300 μL) were taken from the tail vein over the time course 2, 4, 8, 15, 30, 60, 120, 180, 300, 420, 720 and 1440 min. Blood was centrifuged at 1110× *g* for 10 min at 4°C. Plasma was extracted and immediately stored at −20°C for bioanalysis of the plasma concentrations of compound that was performed later.

PK parameters were calculated using non-compartmental analysis in WinNonlin (v. 3.2, Pharsight Corporation, Mountain View, CA, USA).

Onset studies

Two separate studies (onset 1 and 2) with the DPP1 inhibitor AZ1 were performed to investigate the onset of action, that is, the time course for reduction of the activities of the NSPs. Doses were selected based on PK, plasma protein binding (PPB) and *in vitro* DPP1 potency data to ensure that systemic plasma concentrations were maintained at levels expected to inhibit DPP1 by at least 75% throughout the course of the study. In onset 1, AZ1 was administered orally twice daily at 3.6 $mg \cdot kg^{-1}$ in the morning and at 10.7 $mg \cdot kg^{-1}$ 8 h later (to maintain plasma coverage throughout the 24 h period) for 5, 8, 10, 12 and 14 days. The matched vehicle controls (0.1 M citrate buffer, pH 3.0) were treated for 14 days. Once it had been established from study onset 1 that 8 days was sufficient to achieve a maximal response in study onset 2, AZ1 was administered as in onset 1 but for 1, 2, 4, 5 and 8 days and matched vehicle controls were treated twice daily for 8 days.

Recovery study

The aim of this study was to investigate the time course for recovery of the activities of NSPs. The DPP1 inhibitor AZ2 was administered orally as a suspension at 10 mg·kg^{-1} twice daily for 8 days, the first dose in the morning and the second 8 h later. This dose was predicted to ensure a plasma exposure consistent with a high level of DPP1 inhibition. The matched vehicle controls (0.5% Methocel™, 0.1% Tween 80 in citrate buffer, pH 3) were administered twice daily for 8 days. The rats were terminated at 9 day intervals on day 0, 9 or 18 after the end of the treament.

Sampling

On each study day, rats were weighed and the dose adjusted accordingly. Tail vein blood for analysis of compound exposure was taken from the tail of two animals immediately before the morning dose (i.e. 16 h post dose, equal to the trough concentration). The blood was delivered into EDTA tubes, centrifuged at 4°C, and the plasma was saved and stored at −20°C until measurement of compound levels.

Two hours after the last treatment, tail vein blood was collected and added to EDTA tubes for plasma concentration analyses. After tail vein sampling, the animals were anaesthetized with isoflurane, and blood was taken from the vena cava (onset) or via cardiac puncture (recovery), and the femurs were taken from each animal for bone marrow aspirates.

Processing of blood cell lysates

Blood was transferred immediately onto 3% Dextran solution and left for sufficient time to allow separation at room temperature (~20°C). The supernatant was transferred to a fresh tube, and the volume adjusted to 15 mL by adding PBS-Glucose (0.2% w/v). The sample was centrifuged at 800× *g*, and the pellet was resuspended in isotonic NH_4Cl in PBS to allow red blood cell lysis to occur. The sample was centrifuged at 800× *g*, and the cell pellet was resuspended in PBS-Glucose, and cells were counted using a Sysmex XT-2000i (Sysmex, USA). After centrifugation at 10 000× *g*, ice-cold PBS-TX-100 lysis buffer was added to the cell pellet to obtain 10^8 cells mL^{-1}, and the samples were left on ice to allow cell lysis. Lysis volume was calculated for each sample based on total leukocytes in each sample. After cell lysis, the supernatants were kept at −80°C until NSP activity analyses.

Processing of bone marrow cell lysates

Bone marrow cells were extracted from rat femurs using ice-cold air-buffered RPMI (RPMI medium containing 10 mM HEPES, pH 7.4). After centrifugation at 800× *g*, the pellet was resuspended in PBS, and the total number of leukocytes was counted using automated Sysmex XT-2000i. The samples were centrifuged at 800× *g*, and ice-cold lysis buffer (PBS containing 10% (w/v) Triton X-100) was added to the cell pellet to obtain 10^8 cells mL^{-1}, and the samples were left on ice to allow cell lysis. The samples were centrifuged at 10 000× *g*, and the supernatants were kept at −80°C until NSP activity analyses.

Analysis of NSP activities

Bone marrow and blood lysates were added to a 384-well black plate and incubated for 15 min in the presence of a DMSO control (to measure activity within the sample) or NE, PR3 or CatG inhibitor (see above for details, to confirm that the activity measured was due to NE, PR3 or CatG, respectively).

The synthetic substrates were added to the plates, and the resulting fluorescence (at 350–380 nm excitation and 450–460 nm emission for NE; at 320–490 nm excitation and 405–520 nm emission for PR3) or absorbance (at 405 nm for CatG) was quantified. The reaction was read on a Spectramax M5 plate reader (Molecular Devices, Sunnyvale, CA, USA) or a Safire plate reader (Tecan Group Ltd, Switzerland). Reaction kinetics was monitored for up to 60 min for NE and PR3 and for 90–120 min for CatG to ensure that the maximal linear value is reached. The time course data for the non-inhibited wells were plotted in GraphPad Prism® version 5.04 (GraphPad Software Inc., CA, USA), to establish the linear range. The initial rate was calculated using data on the linear range. Points exceeding this range were deleted from the data set for analysis purposes.

Bioanalysis

Plasma concentrations of AZ1 and AZ2 were determined in blood samples collected from *in vivo* rat studies (onset, recovery and PK studies) and PPB studies as detailed below. For AZ1, plasma was dispensed into 50 μL aliquots, and 150 μL of methanol was added (containing internal standard) and mixed. Appropriate standard curves and quality control samples prepared in control rat plasma were used for each analysis. Samples were analysed by LC–MS/MS with an HP1100 HPLC system (Hewlett Packard, Palo Alto, CA) linked to a Quattro Ultima mass spectrometer (Micromass, Waters, Milford, MA) in negative or positive electrospray ionization mode with data analysis on QuanLynx software (version 4.0, Micromass, Waters). Cone voltage and collision energy were optimized for the compound. In these analyses, chromatographic separation was achieved using a Waters Symmetry C8 3.5 μm (2.1 × 30 mm) column using 10 μL of each sample. The mobile phase consisted of an aqueous phase of water with 0.1% (v/v) formic acid and an organic phase of methanol with 0.1% (v/v) formic acid. Samples were quantified using appropriate calibration curves and quality controls.

For AZ2, plasma samples were thawed rapidly and aliquots (50 μL) treated with four volumes (200 μL) of acetonitrile containing carbamazepine as an analytical internal standard. Precipitated proteins were removed by centrifugation, and the supernatant was analysed by ultra-performance liquid chromatography–MS/MS with an ACQUITY® TQD (Waters, Milford, MA). A 2 min gradient from 95% water to 95% acetonitrile, both containing 0.01% formic acid, was used with a Phenomenex Kinetex C18 column. Quantification of the samples was by reference to a calibration line prepared at concentrations from 0.5 to 2000 ng·mL^{-1} in control rat plasma. Concurrently prepared, independent quality control samples, at 8, 80 and 800 ng·mL^{-1}, were used to confirm satisfactory performance of the method during the analytical run.

DPP1 activity cell assay

The potency of the DPP1 inhibitors was investigated by using THP1 cells and a cell permeable fluorogenic substrate, Gly-Phe-AFC as previously described (Thong *et al.*, 2011).

Briefly, cells were incubated with various concentrations of inhibitor for 60 min at 37°C, and the potency (IC_{50}) of the compound in blocking the production of fluorescence product by THP1 cells was calculated. The data were imported into the DataProcessor software package (developed at AstraZeneca Charnwood, UK) for calculation of per cent inhibition. DataProcessor used an open source Java library utilizing the Levenberg–Marquardt algorithm to carry out non-linear least squares fitting using the four-parameter logistic equation:

$$y = A + ((B - A) \div (1 + ((C \div x)\text{^}D)))$$

A is the top of curve, B is the bottom of curve, C is the mid-point of the curve = IC_{50}, D is the slope, x is the independent variable, in this case the concentrations of drug and y is the observed dependent variable, in this case the normalized per cent effect values calculated at each concentration of drug and normalized to the vehicle and maximum inhibition controls. The algorithm is an iterative procedure that aims to give an estimate of the four parameters by generating a best-fit curve through the data that minimize the sum of the squared residuals and find the local minima for each of the four parameters.

Determination of PPB

PPB was measured using equilibrium dialysis in at least three different studies in rat and/or human for each compound. The compounds (final concentration 10 μM) were added to plasma (either rat or human) and placed on one side of a dialysis cell; the other side containing only buffer. The compounds were dialysed through a 5 kD membrane in a Dianorm rotating unit (Diachema, Switzerland) for 18 h at 37°C. Aliquots from the buffer and dialysate side of the membrane were then quenched in methanol and analysed via LC–MS/MS as for the *in vivo* samples.

Prediction of human PK for AZ2

Human PK parameters used in the human simulations were predicted by combining a number of methods. Briefly, absorption was predicted based on *in vitro* experiments using Caco-2 cells to obtain apparent permeability data; the fraction absorbed in the preclinical species (rat and dog) were back-calculated from bioavailability, clearance and hepatic blood flow rates. Because these values were high for AZ2, then a fraction absorbed of one was used. A prediction of metabolic clearance was made from intrinsic clearance measured in human hepatocyte incubations using an *in vitro* to *in vivo* scaling approach (Obach, 1999; Riley *et al.*, 2005; BoChiba *et al.*, 2009). The non-metabolic component of clearance was predicted using allometry from rat and dog renal and biliary clearance (Mahmood, 2005; Paine *et al.*, 2011). Volume of distribution (V_{ss}) was predicted by using a combination of rat and dog V_{ss} and PPB data (Oie and Tozer, 1979). It was calculated using the following equation that had been refined following regression analysis of observed versus predicted human V_{ss} for a series of marketed drugs:

$$\log(Vss_{human}) = 0.9544 \log\left(Vss_{animal}\frac{fu_{human}}{fu_{animal}} + 0.1\left(1 - \frac{fu_{human}}{fu_{animal}}\right)\right) - 0.0565$$

A single compartment model was then used to estimate human $t_{1/2}$. The therapeutic dose was calculated based on the dose predicted to give an average plasma concentration that was equal to 3 × the *in vitro* DPP1 IC_{50} (McGinnity *et al.*, 2007).

Pharmacokinetic/pharmacodynamic modelling of NSP activity in rat

The time course of NSP activity (pharmacological response denoted by R) measured in the rat studies was described by an indirect response model. If DPP1 inhibition is assumed to affect the rate of production of NSP activity, then the rate of change of R is given by

$$\frac{dR}{dt} = k_{in} \times I(C) - k_{out} \times R \quad (1)$$

The parameters k_{in} and k_{out} are the apparent zero-order and first-order rate constants for the production and loss of the response (R). $I(C)$ represents the fraction of uninhibited DPP1 in the presence of a DPP1 inhibitor that will drive the first-order production of NSP activity and is given by

$$I(C) = 1 - \frac{C}{IC_{50} + C} \quad (2)$$

The fraction of DPP1 inhibition (second term in Equation 2) is dependent on the plasma concentration of the DPP1 inhibitor (C) and its potency (IC_{50}). IC_{50} is the concentration needed for 50% inhibition of DPP1 enzyme, based on *in vitro* potency data adjusted to account for the PPB. The steady state NSP activity in the absence of the inhibitor (or base response, R_0) is assumed to be 100%. Therefore, in Equation 1, at t = 0, when no inhibitor is present and $I(C)$ is one, the rate of change of NSP activity is expected to be zero (dR/dt = 0), and the two terms on the right-hand side of the equation are equal to one another, resulting in $R_0 = k_{in}/k_{out}$ = 100%. Thus, k_{in} can be obtained, knowing k_{out}; k_{out} is estimated keeping all other model parameters fixed by fitting the model to the time course of NSP activity observed in blood in the onset study on AZ1 and in bone marrow in the recovery study on AZ2. Temporal changes in exposure during dosing and washout periods in the onset and recovery experiments measuring the NSP activities were simulated for the doses administered using PK parameters of the compounds assuming a one-compartment PK model.

Simulations for AZ2 in man

A human k_{out} was calculated based on the human neutrophil turnover rate of 6.6 days as reported in the literature (Dancey *et al.*, 1976). Based on the predicted human PK parameters for AZ2 as shown in Table 2, the time course of DPP1 inhibition can be obtained as detailed above for the predicted human dose. Combining this with the estimated k_{out}, the time course of the reduction in protease activity was simulated.

All simulations were performed using MATLAB (Release 2014a, The MathWorks, Inc., Natick, MA, USA).

Materials

The DPP1 inhibitor compounds AZ1 ((S)-N-((S)-1-cyano-2-(4′-cyanobiphenyl-4-yl)ethyl)piperidine-2-carboxamide) and AZ2 ((S)-4-amino-N-(1-cyano-2-(4′-cyanobiphenyl-4-yl) ethyl)tetrahydro-2H-pyran-4-carboxamide) were supplied by AstraZeneca R&D (Table 1).

In the onset studies, recombinant human CatG (Calbiochem), NE (Calbiochem) and PR3 (EPC (Elastin Products Company)) were used as positive controls for the substrate. In the recovery study, the CatG inhibitor Cathepsin G inhibitor I (Merck Millipore), the NE inhibitor AZ12757277 (WO20 11039528) and the PR3 inhibitor Sivelestat (WO2000052032) were used to confirm that the activity measured was due to CatG, NE and PR3 respectively. The synthetic substrates used were N-succinyl-Ala-Ala-Pro-Phe-pNA for CatG (Sigma), Methoxysuccinyl-Ala-Ala-Pro-Val-AMC for NE (Sigma) and 5-FAM-L2p-Tyr-Asp-Lys-Gly-Asp-Arg-Lys(QXL520)-NH_2 for PR3 in the onset studies (Anaspec), or (7-Methoxycoumarin-4-yl)acetyl-lysyl-(picolinoyl)-Tyr-Asp-Ala-Lys-Gly-Asp-N-3-(2–4-dinitrophenyl)-2–3-diaminopropyonyl-NH_2 for PR3, in the recovery study (Peptide Synthetics).

Results

NSP activities observed in rat blood and bone marrow

In onset 1 (14 day study), the maximum reduction in NE and PR3 activities in bone marrow was reached after 8 days of treatment with a DPP1 inhibitor (AZ1) to naive rats (Figure 1a and b). Similar results were obtained in blood (Figure 1c and d). In the 8 day study (onset 2), the reduction in NE and PR3 activities following the oral administration of the DPP1 inhibitor, AZ1, showed a more uniform trend in blood (Figure 1e and f) than in bone marrow (not shown) and were therefore preferred for parameter estimation using the indirect response model. The assay window for measuring CatG activity was small due to the colorimetric nature of the assay, and it was difficult to determine a trend of decreasing activity. The maximal inhibition of NSP activity ranged from 64% reduction in PR3 activity to 79% reduction in NE activity, which was in agreement with a predicted DPP1 inhibition of 75% at steady state average concentration, based on coverage and *in vitro* potency. Figure 2a–c shows the recovery of the NE, PR3 and CatG activities in bone marrow on day 0, day 9 and day 18 after stopping administration of the DPP1 inhibitor (AZ2) or vehicle. Similar patterns were observed for the recovery of NE, PR3 and CatG activities.

Estimation of k_{out} from the observed NSP activities in onset and recovery studies in rat

The observed and simulated exposure profiles of AZ1 and AZ2 in rat and the corresponding changes in DPP1 inhibition expected based on *in vitro* DPP1 potency data adjusted for PPB are shown in Figures 3a and b and 4a respectively. The exposure profile simulated using the PK parameters appears to agree well with the observed data (Figure 3a and 4a). The indirect response model adequately describes the observed protease activities in both the onset and recovery studies (Figures 3c and 4b). The k_{out} estimated using the onset and recovery data for AZ1 and AZ2 was 0.0072 and 0.0102 h^{-1} respectively. These correspond to a turnover rate of 5.78 days for AZ1 in blood and 4 days for AZ2 in the bone marrow. The residence time ($1/k_{out}$) in the bone marrow is similar to the rat neutrophil turnover time of about 3.75 days that has been reported (Muksinova *et al.*, 1976). The PK and PD parameters employed in the model for the two compounds are presented in Table 2.

Simulations for AZ2 in man

The predicted human PK parameters that were employed as input in the indirect response model for AZ2 are presented in Table 2. A human k_{out} value of 0.0069 h^{-1} was calculated based on a human neutrophil turnover rate of 6.6 days (Dancey *et al.*, 1976). Figure 5a shows the simulated time course of protease activity in human employing this k_{out} in the indirect response model. According to the model, for the clinical dose selected, it would take 7 days to achieve a 50% reduction of protease activity with a maximum reduction of 75% reached after ~20 days of treatment. Using this model, the effects of a missed dose in the clinic were simulated for AZ2 (Figure 5b). A negligible reduction of ~3% in the pharmacological response would be anticipated. A simulation of the washout period following the discontinuation of the DPP1 inhibitor after the maximum reduction in

Table 1

Chemical structures of the DPP1 inhibitor compounds AZ1 and AZ2

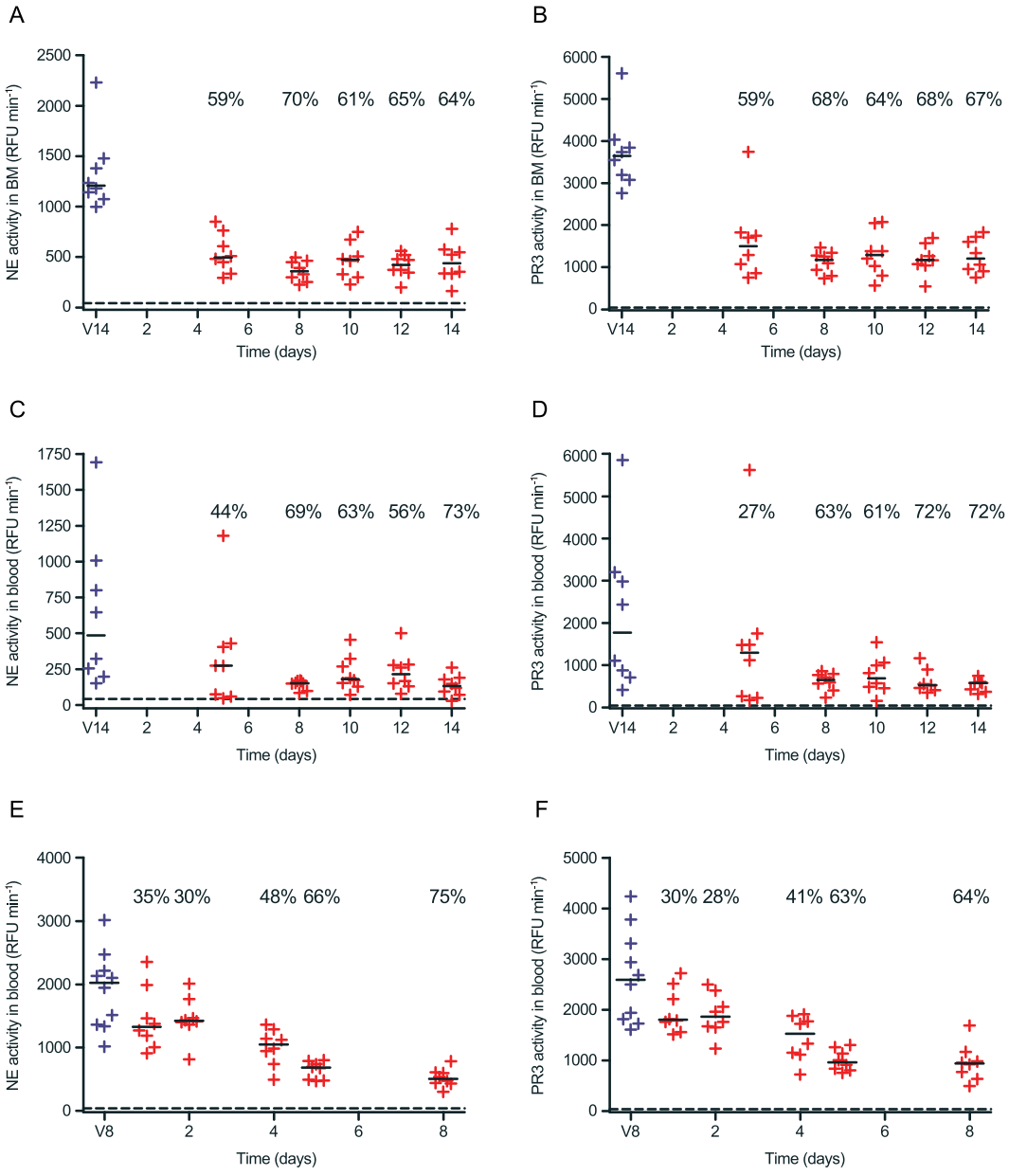

Figure 1

Time course for onset of inhibition of NE and PR3 activities in blood and bone marrow after oral administration of the DPP1 inhibitor AZ1 to rats, (a–d) NE and PR3 activities in bone marrow and blood in onset 1, (e and f) NE and PR3 activities in blood in onset 2. The horizontal lines represent the median value in each group, the percent inhibition is the median value in the respective group compared with the median value in the vehicle-treated group, the dotted line represents the buffer signal, V = vehicle and BM = bone marrow.

protease activity is reached (Figure 5c), shows that the recovery of 50% neutrophil activity would take ~5 days. A return to baseline levels would be expected to take ~25 days.

Discussion

The purpose of the modelling work presented here is to demonstrate that it is reasonable to conclude, from the experimental data presented and the scientific understanding of the biological system in question, that neutrophil maturation and turnover is a key determinant of rate of change in NSP activity. Central to the hypothesis is the interconnected nature of neutrophil maturation and the processing of pre-NSPs by DPP1 to their active form only at a specific promyelocyte stage of neutrophil maturation (Figure 6). This has been described in detail in several papers and reviews (Fouret *et al.*, 1989; McGuire *et al.*, 1993; Garwicz *et al.*, 1997; Guay *et al.*, 2010; Korkmaz *et al.*, 2010). It has also been reported that in subjects lacking DPP1 (e.g. with Papillon–Lefèvre Syndrome), pre-NSPs are degraded before neutrophils are sufficiently mature to be released into the

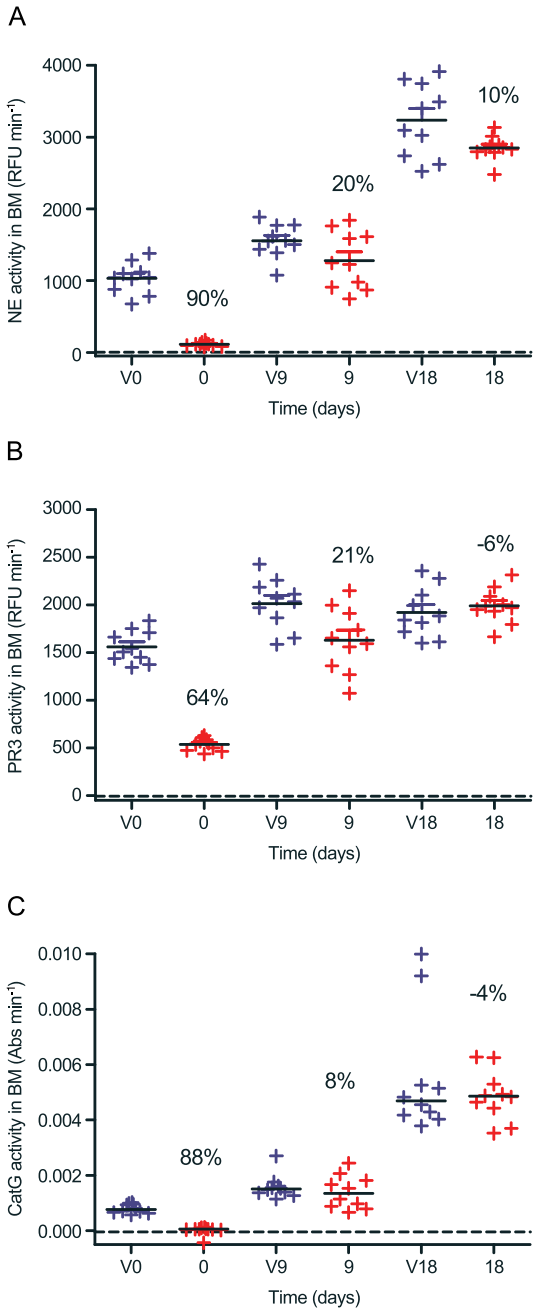

Figure 2

Time course for recovery of (a) NE, (b) PR3 and (c) CatG activities in bone marrow in AZ2-treated and vehicle-treated (control) rats. The DPP1 inhibitor AZ2 or vehicle control was administered orally twice daily for 8 days, the first dose in the morning and the second 8 h later. The rats were killed at 9 day intervals on day 0, 9 or 18 after the end of the treatment. The horizontal line represents the median value in each group, the percent inhibition is the median value in the respective group compared with the median value in the matched vehicle-treated group, the dotted line represents the buffer signal, V = vehicle and BM = bone marrow.

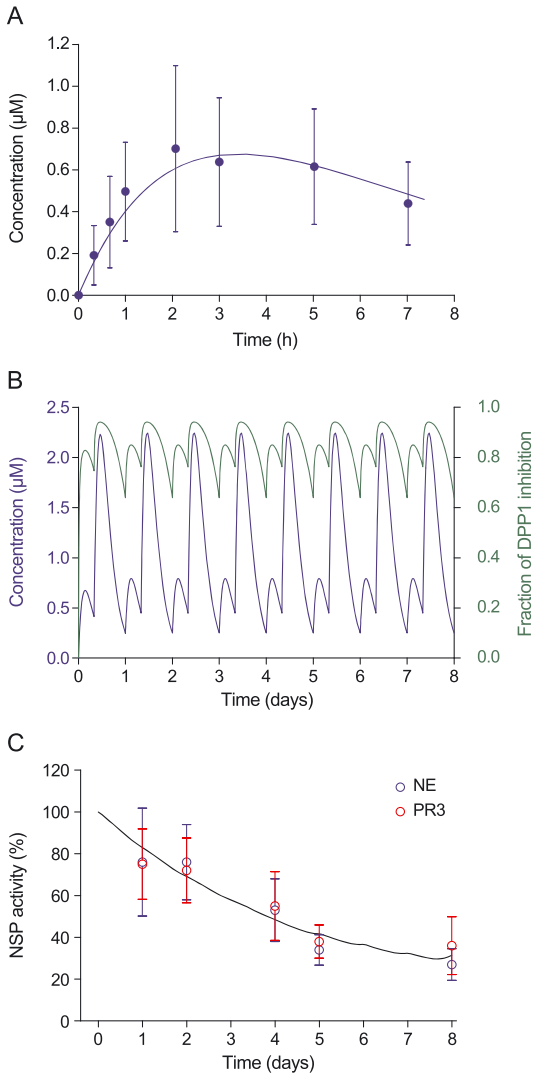

Figure 3

(a) Simulated time course of concentration of AZ1 after an oral dose (3.6 mg·kg^{-1}) in rat with markers showing dose-adjusted observed pharmacokinetic data, 0–8 h. (b) Simulated time course of concentration of AZ1 and fraction of DPP1 inhibition after twice daily oral dose (3.6 mg·kg^{-1} and 10.7 mg·kg^{-1} after 8 h) in rat 0–8 days. (c) Best fit to the observed time course of NSP inhibition after oral administration of AZ1 in the onset study. Note: observed CatG inhibition data from the onset study were not included in the fitting.

circulation, indicating that pre-NSP processing in the mature neutrophil is unlikely (Sorensen *et al.*, 2014). Consequently, DPP1 inhibition most likely acts by decreasing the amount, and resulting activity, of NSPs only in newly formed neutrophils in the bone marrow.

The indirect response model in rat adequately described the observed reduction in NSP activity following oral administration of a DPP1 inhibitor. Assuming that the time taken to attain maximum reduction in protease activity in rat bone marrow is driven by the neutrophil turnover rate, the first-order rate constant, k_{out} estimated from the best fit of all observed AZ2 data to the model, corresponds to a mean rat neutrophil turnover time of 4 days, which is similar to the residence time of 3.75 days for maturing non-dividing neutrophils in the bone marrow for rat that has been reported previously (Muksinova *et al.*, 1976). The k_{out} estimated using

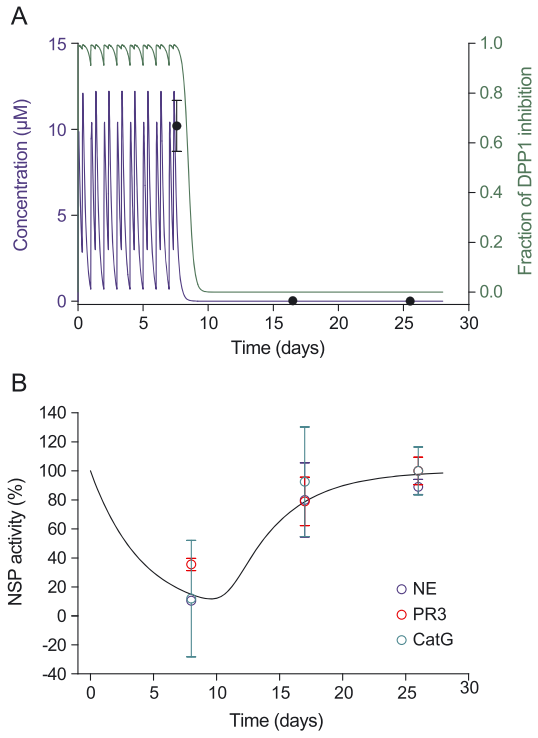

Figure 4

(a) Simulated time course of concentration of AZ2 and fraction of DPP1 inhibition after twice daily oral administration (10 mg·kg^{-1}) in rat. Markers show exposure data in rats in the recovery study. (b) Best fit to the observed time course of NSP inhibition after oral administration of AZ2 in the recovery study in rat.

only onset study data in blood corresponds to a residence time of 5.78 days (Table 2). This slower kinetics in blood is perhaps a reflection of the delay introduced by maturation and release of neutrophil from bone marrow into blood. The difference of 1.78 days then corresponds to an average lag time between bone marrow and blood. Therefore, modelling of the rat data supports the hypothesis that the turnover of neutrophils is a major driver of NSP activity following DPP1 inhibition. While it is possible that NSP degradation is a factor regulating NSP activity, this is not supported by the data generated by us and presented here, because this would extend the estimate of turnover time further in order for the model to describe the data and, as noted above, this is already slightly longer than the previously reported value of 3.75 days (Muksinova *et al.*, 1976). It therefore seems unlikely that NSP degradation plays a major role in regulating NSP activity in this study.

In the rat, a good correlation is evident between *in vitro* IC_{50} for DPP1 inhibition and the extent of reduction of NSP activity observed *in vivo* in bone marrow or blood. Thus, the maximum reduction in protease activity in blood seen with AZ1 in the onset studies is about 75%, as expected from the 75% inhibition of DPP1 enzyme activity by AZ1, whereas, the maximum reduction in protease activity observed with AZ2 in bone marrow in the recovery study is 90%, in keeping with the near-complete inhibition of DPP1 by AZ2 (Figures 3 and 4). However, other workers have found that NSP activity is reduced by less than the level of DPP1 inhibition (Méthot *et al.*, 2008). In addition, the fractional inhibition may also vary between different species and *in vitro* cell systems that may lead to an altered correlation in human to the one that we have observed in the rat. Nevertheless, the rat data presented here strengthens confidence in the use of human *in vitro* DPP1 inhibition data for predicting the extent of reduction in the NSP activity that can be expected *in vivo*.

Although there was a good agreement between the level of *in vitro* DPP1 inhibition and reduction of NSP activity *in vivo*, it was not possible to measure a decrease in CatG activity in the onset studies. However, in separate in-house studies (not part of this work), inhibition of CatG has been demonstrated. This lack of effect on CatG activity in the two onset studies with AZ1 may be because the assay window for measuring CatG activity was small due to the colorimetric nature of the assay and it was difficult to determine a trend of decreasing activity. Nevertheless, this was satisfactorily addressed in the recovery study where the inhibition of CatG activity and its recovery was clearly shown. In general, NSP activity measurements were more robust in bone marrow

Table 2

Parameters employed in the indirect response model

		PK parameters[a]				Indirect response model parameters	
	Species	CL (L·h^{-1})	V_{ss} (L·kg^{-1})	*F* (%)	PPB[b] (%free)	[c]DPP1 IC_{50} (μM)	[d]k_{out} (h^{-1}) (95% CI)
AZ1	Rat	0.4	5.6	80	4.1	0.14	0.0072 (0.0060–0.0083)
AZ2	Rat	0.1	1.9	92	11	0.067	0.0102 (0.0069–0.014)
AZ2	Human	3.4	1.3	96	9.1	0.044	0.0069

[a]CL, V_{ss} and *F* observed mean values in rat (*n* of at least 4), mean CL observed in single dose PK experiments (0.25 and 0.14 L·h^{-1} for AZ1 and AZ2, respectively) were adjusted slightly to fit plasma concentrations observed in animals in onset and recovery studies. Human values predicted as described in Methods.
[b]Mean value (*n* of at least 3).
[c]Corrected for PPB.
[d]Estimated by fitting the indirect response model to the observed NSP activities in rat and calculated using neutrophil turnover time in human.
CL, clearance; V_{ss}, volume of distribution at steady state; *F*, oral bioavailability; PPB, plasma protein binding; IC_{50}, concentration needed for 50% inhibition; k_{out}, first-order rate constant for loss of response; CI, confidence interval.

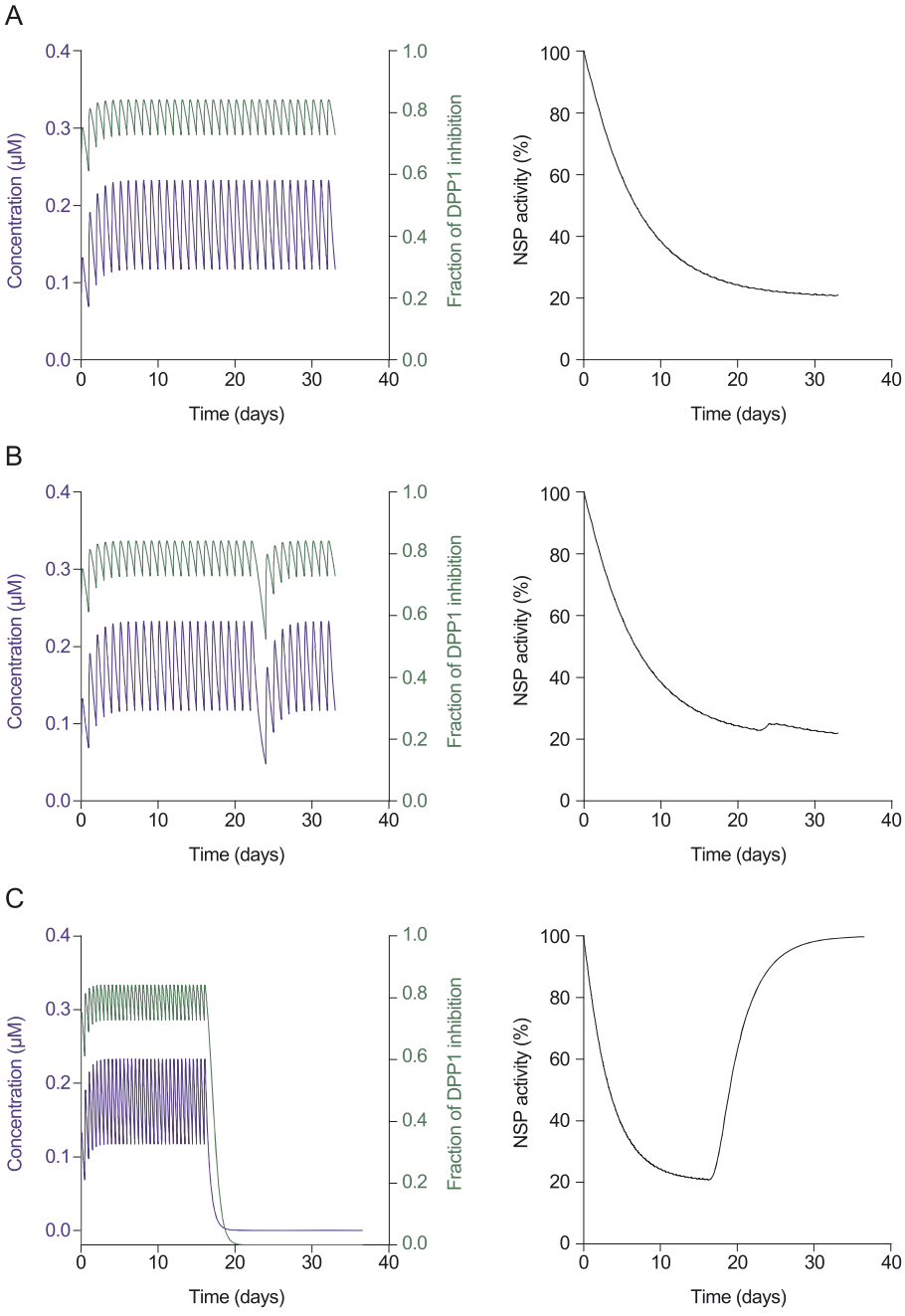

Figure 5

(a) Left-hand panel shows simulated time course of concentration of AZ2 and fraction of DPP1 inhibition following once daily oral administration in human at a dose that is predicted to give a steady state average concentration of 3 × IC_{50} and inhibits DPP1 by 75%. Right-hand panel shows simulated time course of NSP inhibition in human after oral administration of AZ2. (b) Simulated effect of a missed dose on day 24 (typically after steady state is reached). (c) Simulated recovery of NSP activity following the discontinuation of treatment with AZ2.

than in blood. This may be because rat bone marrow is a richer source of neutrophils, thereby ensuring a wider assay window. However, in the onset studies, it was possible to show that the bone marrow changes in NSP activity are reflective of the changes seen in blood.

It was interesting to find that, like the reduction of NSP activity in the rat, the rate of recovery on cessation of treatment was also consistent with the neutrophil turnover rate (Figure 4b). This indicates that the NSPs are not stored in more mature neutrophils in a precursor format that can be quickly activated when DPP1 inhibition is removed, but that NSPs are activated by DPP1 only during the promyelocyte stage of neutrophil maturation. This is consistent with the findings of Sorensen *et al.*, where the pro-NSPs were shown to be degraded before the neutrophils were fully mature and reached the blood circulation (Sorensen *et al.*, 2014).

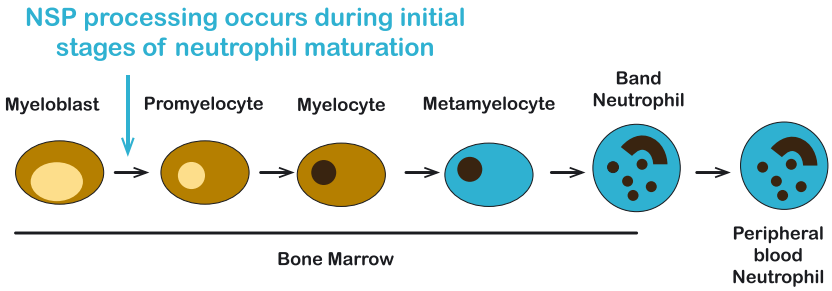

Figure 6
Illustration of neutrophil maturation and when NSP processing is thought to occur (modified from Bekkering and Torensma, 2013).

However, some previously published data using *in vitro* systems had implied that this may not be the case (Méthot *et al.*, 2007) and that pro-NSPs stored intracellularly could be rapidly processed in the absence of DPP1 inhibition leading to a rapid recovery of activity. The difference in NSP recovery rates observed may highlight the difficulties in extrapolating from *in vitro* systems to *in vivo*.

AZ2 was chosen to simulate the time course of NSP inhibition in human based on predicted PK parameters, measured *in vitro* DPP1 inhibition, and published neutrophil turnover rate in human (Dancey *et al.*, 1976). As shown in Figure 5, the time needed to observe maximum reduction (in this case 75%) in NSP activity in human bone marrow is predicted to be 20–25 days (i.e. four to five times the turnover of neutrophils). Based on results from the rat, an additional lag time may be needed when sampling in blood. If, as shown in the rat, neutrophil turnover rate is a key determinant of the rate of change of NSP activity in human, it is important to consider the resulting delayed onset of inhibition when designing clinical trials, and dosing may need to be extended to allow the full effects of a DPP1 inhibitor on NSP activity. NSPs themselves should act as useful biomarkers in understanding this effect. For example, it should be relatively straightforward to monitor the NSP activity and DPP1 inhibition in blood in early phase 1 clinical trials using established techniques (Stevens *et al.*, 2011; Romero-Quintana *et al.*, 2013). Such readily accessible biomarkers should enable good evidence of proof of mechanism to be achieved early in the development process for a suitable DPP1 inhibitor candidate drug. While it is theoretically possible to sample directly from the bone marrow – because this is the targeted tissue compartment – this would obviously involve a much more invasive sampling regime. However, the evidence presented in this work suggests that the blood is a reasonable surrogate, particularly considering the therapeutically beneficial consequences of DPP1 inhibition are likely to rely on a reduction of NSP activity in the blood, subsequently reducing NSP activity at the site of inflammation. Moreover, there may also be good opportunity to monitor NSP activity in the tissue or site of inflammation, as done by other workers when investigating effects of NE inhibition on sputum NE levels in patients with cystic fibrosis (Elborn *et al.*, 2012).

It is reassuring that the simulation of missing a dose of a once daily DPP1 inhibitor shows only a minimal impact on NSP activity (Figure 5b). Indeed, because of the longer neutrophil turnover rate in human, it is predicted that the NSP activity recovery would be even more modest than observed in rat. If the human simulations are predictive, then this suggests that poor patient compliance may not be a major issue in this regard with drugs that aim to reduce NSP activity via this mechanism. However, these simulations also suggest that it may be important to continue to monitor subjects after cessation of treatment, because recovery of NSP activity is predicted to be gradual.

Preclinical modelling to optimize early clinical development studies so that the primary objectives of safety and tolerability can be supplemented with high value information about the target and target engagement should be very useful, particularly when embarking on the development of unprecedented targets such as DPP1. The role of neutrophil biology in the context of human lung disease is not yet fully elucidated, and the evaluation of the effects of DPP1 inhibition on clinical outcome in patients will provide a novel and exciting opportunity to dissect out whether NSPs have a pathogenic role in respiratory diseases such as COPD.

Acknowledgements

We would like to thank the DPP1 project team at the former AstraZeneca R&D Charnwood site and those involved at AstraZeneca R&D Mölndal for their assistance in completing this work.

Author contributions

P.G., C.W., S.C., J.S., A.B. and S.A.P. wrote the manuscript, designed the research, performed the research and analysed the data.

Conflict of interest

The authors declare no conflicts of interest.

Declaration of transparency and scientific rigour

This Declaration acknowledges that this paper adheres to the principles for transparent reporting and scientific rigour of

preclinical research recommended by funding agencies, publishers and other organisations engaged with supporting research.

References

Alexander SPH, Fabbro D, Kelly E, Marrion N, Peters JA, Benson HE *et al.* (2015). The concise guide to PHARMACOLOGY 2015/16: Enzymes. Br J Pharmacol 172: 6024–6109.

Bekkering S, Torensma R (2013). Another look at the life of a neutrophil. World J Hematol 2: 44–58.

BoChiba M, Ishii Y, Sugiyama Y (2009). Prediction of hepatic clearance in human from *in vitro* data for successful drug development. AAPS J 11: 262–276.

Dancey JT, Deubelbeiss KA, Harker LA, Finch CA (1976). Neutrophil kinetics in man. J Clin Invest 58: 705–715.

Elborn JS, Perrett J, Forsman-Semb K, Marks-Konczalik J, Gunawardena K, Entwistle N (2012). Efficacy, safety and effect on biomarkers of AZD9668 in cystic fibrosis. Eur Respir J 40: 969–976.

Fouret P, du Bois RM, Bernaudin JF, Takahashi H, Ferrans VJ, Crystal RG (1989). Expression of the neutrophil elastase gene during human bone marrow cell differentiation. J Exp Med 169: 833–845.

Fox S, Leitch AE, Duffin R, Haslett C, Rossi AG (2010). Neutrophil apoptosis: relevance to the innate immune response and inflammatory disease. J Innate Immun 2: 216–227.

Friberg LE, Henningsson A, Maas H, Nguyen L, Karlsson MO (2002). Model of chemotherapy-induced myelosuppression with parameter consistency across drugs. J Clin Oncol 20: 4713–4721.

Fujita J, Nelson NL, Daughton DM, Dobry CA, Spurzem JR, Irino S *et al.* (1990). Evaluation of elastase and antielastase balance in patients with chronic bronchitis and pulmonary emphysema. Am Rev Respir Dis 142: 57–62.

Furber M, Tiden A, Gardiner P, Mete A, Ford R, Millichip I *et al.* (2014). Cathepsin C inhibitors: Property optimization and identification of a clinical candidate. J Med Chem 57: 2357–2367.

Garwicz D, Lindmark A, Hellmark T, Gladh M, Jögi J, Gullberg U (1997). Characterization of the processing and granular targeting of human proteinase 3 after transfection to the rat RBL or the murine 32D leukemic cell lines. J Leukoc Biol 61: 113–123.

Guay D, Beaulieu C, David Percival M (2010). Therapeutic utility and medicinal chemistry of cathepsin C inhibitors. Curr Top Med Chem 10: 708–716.

Keatings VM, Collins PD, Scott DM, Barnes PJ (1996). Differences in interleukin-8 and tumor necrosis factor-alpha in induced sputum from patients with chronic obstructive pulmonary disease or asthma. Am J Respir Crit Care Med 153: 530–534.

Kilkenny C, Browne W, Cuthill IC, Emerson M, Altman DG (2010). Animal research: reporting *in vivo* experiments: the ARRIVE guidelines. Br J Pharmacol 160: 1577–1579.

Kolaczkowska E, Kubes P (2013). Neutrophil recruitment and function in health and inflammation. Nat Rev Immunol 13: 159–175.

Korkmaz B, Horwitz MS, Jenne DE, Gauthier F (2010). Neutrophil elastase, proteinase 3, and cathepsin G as therapeutic targets in human diseases. Pharmacol Rev 62: 726–759.

Lalonde R, Kowalski K, Hutmacher M, Ewy W, Nichols D, Milligan P *et al.* (2007). Model-based drug development. Clin Pharmacol Ther 82: 21–32.

Mahmood I (2005). Interspecies scaling of biliary excreted drugs: a comparison of several methods. J Pharm Sci 94: 883–892.

McGinnity D, Collington J, Austin R, Riley R (2007). Evaluation of human pharmacokinetics, therapeutic dose and exposure predictions using marketed oral drugs. Curr Drug Metab 8: 463–479.

McGrath JC, Lilley E (2015). Implementing guidelines on reporting research using animals (ARRIVE etc.): new requirements for publication in BJP. Br J Pharmacol 172: 3189–3193.

McGuire MJ, Lipsky PE, Thiele DL (1993). Generation of active myeloid and lymphoid granule serine proteases requires processing by the granule thiol protease dipeptidyl peptidase I. J Biol Chem 268: 2458–2467.

Méthot N, Guay D, Rubin J, Ethier D, Ortega K, Wong S *et al.* (2008). *In vivo* inhibition of serine protease processing requires a high fractional inhibition of cathepsin C. Mol Pharmacol 73: 1857–1865.

Méthot N, Rubin J, Guay D, Beaulieu C, Ethier D, Reddy TJ *et al.* (2007). Inhibition of the activation of multiple serine proteases with a cathepsin C inhibitor requires sustained exposure to prevent pro-enzyme processing. J Biol Chem 282: 20836–20846.

Milligan P, Brown M, Marchant B, Martin S, van der Graaf P, Benson N *et al.* (2013). Model-based drug development: a rational approach to efficiently accelerate drug development. Clin Pharmacol Ther 93: 502–514.

Muksinova KN, Murzina LD, Sukhodoev VV (1976). Kinetics of cell populations in the compartment of maturing, non-dividing neutrophils of rat bone marrow. Biull Eksp Biol Med 82: 986–987.

Obach RS (1999). Prediction of human clearance of twenty-nine drugs from hepatic microsomal intrinsic clearance data: an examination of *in vitro* half-life approach and nonspecific binding to microsomes. Drug Metab Dispos 27: 1350–1359.

Oie S, Tozer TN (1979). Effect of altered plasma protein binding on apparent volume of distribution. J Pharm Sci 68: 1203–1205.

Paine SW, Menochet K, Denton R, McGinnity DF, Riley RJ (2011). Prediction of human renal clearance from preclinical species for a diverse set of drugs that exhibit both active secretion and net reabsorption. Drug Metab Dispos 39: 1008–1013.

Pillay J, den Braber I, Vrisekoop N, Kwast LM, de Boer RJ, Borghans JA *et al.* (2010). *In vivo* labeling with 2H2O reveals a human neutrophil lifespan of 5.4 days. Blood 116: 625–627.

Riley RJ, McGinnity DF, Austin RP (2005). A unified model for predicting human hepatic, metabolic clearance from *in vitro* intrinsic clearance data in hepatocytes and microsomes. Drug Metab Dispos 33: 1304–1311.

Romero-Quintana JG, Frias-Castro LO, Arambula-Meraz E, Aguilar-Medina M, Duenas-Arias JE, Melchor-Soto JD *et al.* (2013). Identification of novel mutation in cathepsin C gene causing Papillon–Lefevre syndrome in Mexican patients. BMC Med Genet 14: 7. doi:10.1186/1471-2350-14-7.

Sinden NJ, Baker MJ, Smith DJ, Kreft J, Dafforn TR, Stockley RA (2014). Alpha-1-antitrypsin variants and the proteinase/anti-proteinase imbalance in chronic obstructive pulmonary disease. Am J Physiol Lung Cell Mol Physiol . doi:10.1152/ajplung.00179.2014.

Sorensen OE, Clemmensen SN, Dahl SL, Ostergaard O, Heegaard NH, Glenthoj A *et al.* (2014). Papillon–Lefevre syndrome patient reveals species-dependent requirements for neutrophil defenses. J Clin Invest 124: 4539–4548.

Southan C, Sharman JL, Benson HE, Faccenda E, Pawson AJ, Alexander SPH *et al*. (2016). The IUPHAR/BPS Guide to PHARMACOLOGY in 2016: towards curated quantitative interactions between 1300 protein targets and 6000 ligands. Nucleic Acids Res 44 (Database Issue): D1054–D1068.

Stevens T, Ekholm K, Granse M, Lindahl M, Kozma V, Jungar C *et al*. (2011). AZD9668: pharmacological characterization of a novel oral inhibitor of neutrophil elastase. J Pharmacol Exp Ther 339: 313–320.

Stockley R (1994). The role of proteinases in the pathogenesis of chronic bronchitis. Am J Respir Crit Care Med 150: S109.

Thong B, Pilling J, Ainscow E, Beri R, Unitt J (2011). Development and validation of a simple cell-based fluorescence assay for dipeptidyl peptidase 1 (DPP1) activity. J Biomol Screen 16: 36–43.

Wright HL, Moots RJ, Bucknall RC, Edwards SW (2010). Neutrophil function in inflammation and inflammatory diseases. Rheumatology (Oxford) 49: 1618–1631.